Progress In Electromagnetics Research, Vol. 110, 421–435, 2010

UNEQUALLY SPACED AND EXCITED RESONANT SLOTTED-WAVEGUIDE ANTENNA ARRAY BASED ON AN IMPROVED RESONANT-SLOT COUPLED CAVITY CHAIN COMPOSITE RIGHT/LEFT-HANDED WAVEGUIDE

Y. Chen, S. W. Liao, and J. Wei

School of Electronic Engineering
University of Electronic Science and Technology of China
No. 4, Section 2, North Jianshe Road, Chengdu, China

J. H. Xu

School of Physical Electronics
University of Electronic Science and Technology of China
No. 4, Section 2, North Jianshe Road, Chengdu, China

Abstract—This paper presents a new unequally spaced and excited resonant slotted-waveguide antenna array. It is realized by employing an improved resonant-slot coupled cavity chain composite right/left-handed (CRLH) waveguide. As the CRLH waveguide works at the infinite wavelength frequency, all the slot elements along the waveguide wall are excited in-phase. Thus both the element spacings and excitation amplitudes are introduced into the synthesis to realize a resonant slotted-waveguide antenna array. A seven-element unequally spaced and excited antenna array which generates pencil beam is synthesized, simulated and fabricated. The results show, with comparison to the equally spaced but unequally excited resonant slotted-waveguide antenna array, the proposed unequally spaced and excited array produces a lower peak sidelobe level (PSLL).

Received 19 October 2010, Accepted 18 November 2010, Scheduled 26 November 2010
Corresponding author: Ying Chen (chenying3612@hotmail.com).

1. INTRODUCTION

Composite right/left-handed (CRLH) waveguide, as a new type of CRLH transmission line (TL) or one-dimension negative refractive index media [1, 2], is attracting more and more attentions [3–6]. As compared to the planar CRLH TL [7, 8], CRLH waveguide has low loss characteristic and high power handling capability. Planar CRLH TL has many applications in microwave device and antenna [9–12], however the applications of CRLH waveguide are rare. Recently, a novel unequally spaced resonant slotted-waveguide antenna array based on the infinite wavelength propagation property of CRLH waveguide was proposed in our previous paper [13]. For the conventional resonant slotted-waveguide antenna array which has a broadside operation, the slots are located in the guide to achieve a uniform phase distribution. With that being said, a uniform phase distribution is achieved by locating the slots half the guide wavelength ($\lambda_g/2$) apart and placing every other slot on the adjacent side of broadside wall center line. Nonetheless as shown in our previous paper [13], if the CRLH waveguide works at the infinite wavelength frequency, the slots cut anywhere along the CRLH waveguide wall can all be excited in-phase. Consequently unequal spacings with equiamplitude were introduced into the array synthesis for sidelobe reduction.

The result in [13] is formidable, but the main drawback is that the use of CRLH waveguide, itself, is very complicated, and new difficulties may be found when attempting manufacturing of CRLH waveguide [14]. On the other hand, the amplitudes of each slot, as other degrees of freedom available, are useful to achieve further performance improvements [15, 16].

In this paper, an improved resonant-slot coupled cavity chain CRLH waveguide is proposed. As compared with the previous resonant-slot coupled cavity chain CRLH waveguide, the improved CRLH waveguide comprises of only one resonant slot and this makes the structure more compact and simpler. In addition, the proposed CRLH waveguide can be easily excited by rectangular waveguide through the resonant slot.

By employing the improved resonant-slot coupled cavity chain CRLH waveguide, a new unequally spaced and excited resonant slotted-waveguide antenna array is proposed, as shown in Fig. 1. Both the spacings and excitations are introduced into the synthesis for performance improvements (such as peak sidelobe level (PSLL) reduction). A seven-element unequally spaced and excited antenna array which generates pencil beam is synthesized, simulated and

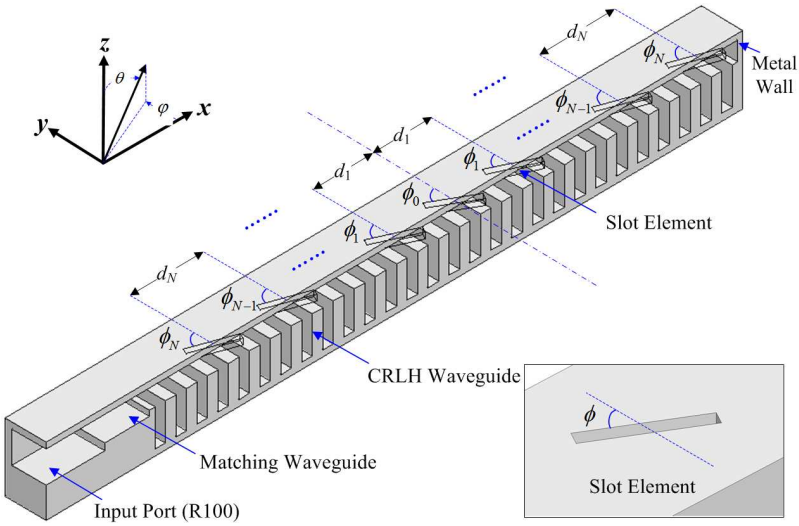

Figure 1. Longitudinal section of an unequally spaced and excited resonant slotted-waveguide antenna array employing the proposed CRLH waveguide. Centered rotated slots, symmetrically situated and excited, are used here, and one of them is shown in the inset. The antenna array is excited by an end-fed structure. d_i and ϕ_i ($i = 1, 2, \ldots, N$) represent the ith adjacent element spacing, and the ith slot rotation angle with respect to the y-axis, respectively.

fabricated. Unlike our previous paper [13], this paper uses a seven-element equally spaced but unequally excited resonant slotted-waveguide antenna array for comparison. With comparison to this equally spaced array, the results show that the proposed unequally spaced and excited array produces a better pattern performance (lower PSLL).

2. IMPROVED RESONANT-SLOT COUPLED CAVITY CHAIN CRLH WAVEGUIDE

2.1. Structure of Improved CRLH Waveguide

The CRLH waveguide structure used in [13] is based on identical symmetrical resonant-slot coupled cavity unit. It was first proposed in [4], and has a similar circular resonant-slot form which has been analyzed by Allen [17]. Allen's theory illustrated that one resonant slot in each unit cell can exhibits shunt inductance and series capacitance, which are necessary for left-handed (LH) propagating waves. However,

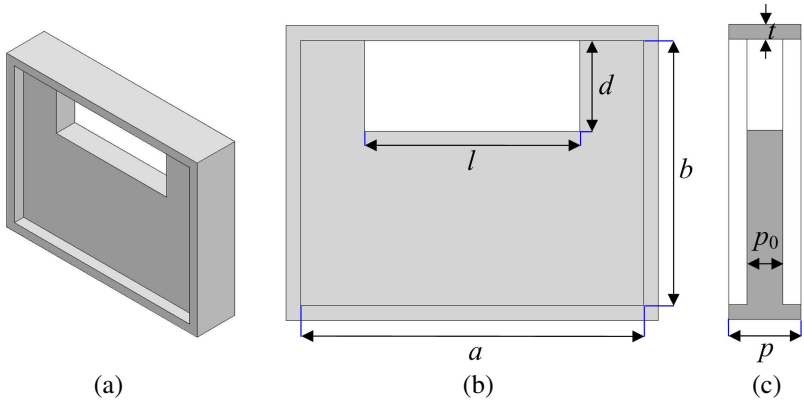

Figure 2. Structure of the improved CRLH waveguide unit cell. ($a = 23.4\,\text{mm}$, $b = 18.1\,\text{mm}$, $l = 14.65\,\text{mm}$, $d = 6.2\,\text{mm}$, $p = 5\,\text{mm}$, $p_0 = 2.5\,\text{mm}$ and $t = 1\,\text{mm}$). (a) General view. (b) Front view. (c) Side view.

more resonant slots, around three to four, are required to increase the couplings among unit cells. To make the structure simple, we consider removing the other three resonant slots, and thus only one resonant slot would remain to maintain LH propagating waves. On the other hand, the thickness of resonant slot is too thin compared with the period length, so it is sensitive to the manufacturing variations and may cause some fabrication problems [14]. In this paper, the thickness of resonant slot is designed to be thicker, and this makes the prototype easier for shaping. The geometry and parameters of one unit cell of the improved resonant-slot coupled cavity chain CRLH waveguide are shown in Fig. 2.

As for the balanced case [1], we briefly describe how we came to the conclusion. According to [18], for this resonant-slot couple cavity structure, there are two passband modes: The slot mode and the cavity mode. To achieve a balanced case, the upper cutoff frequency of slot mode f_s should be equal to the lower cutoff frequency of cavity mode f_c. For the upper cutoff frequency of the slot mode f_s, it is pretty close to the resonant frequency of the slot, hence it is mainly determined by the slot length [18]. The design procedure for the balanced case is: To start, the slot length is chosen at first ($l \approx \lambda_0/2$), making sure that f_s is close to the desired frequency (10 GHz in this letter). Then the period length p is selected and the slot thickness p_0 is designed to be thicker, as stated above. The other parameters, the dimensions of the cavity area ($a \times b$), are tuned at last, aiming to change the frequency

f_c, and making it equal to the frequency f_s. By this means, a balanced case can be achieved.

2.2. Analysis of Equivalent Circuit Model

In [4], the resonant-slot coupled cavity chain CRLH unit cell has been analyzed by field theory. However, this theory is not applicable for this improved structure, since some parameters don't satisfy the conditions like $d \ll \lambda_0/2$ and $d \ll a$ [4]. In this section, another explanation to this improved CRLH waveguide unit cell based on equivalent circuit model is proposed. Although it is not accurate enough, this explanation gives another perspective to qualitatively analyze this CRLH waveguide.

The unit cell shown in Fig. 2 (unit cell B) has another equivalent form (unit cell A), which is shown in Fig. 3. Actually, if two sections of unit cell B are connected together, the center half of these two unit cells is unit cell A. The unit cell A can be decomposed into three parts, which are a section of rectangular waveguide, corrugations on both sidewalls and a short-ended stub attached on the bottom wall of the rectangular waveguide, respectively. There are also three component parts for the equivalent circuit model correspondingly, as shown in Figs. 4(a), (b) and (c). Equivalent circuit of unit cell is shown in Fig. 4(d).

For the rectangular waveguide, it introduces a per-unit-length series inductance L_w and shunt capacitance C_w when operating

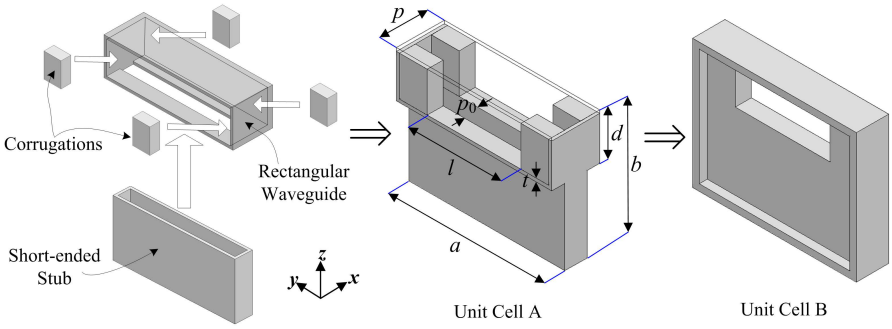

Figure 3. Another equivalent form of the proposed CRLH waveguide unit cell. It is composed of a section of rectangular waveguide, corrugations on both sidewalls and a short-ended stub on the bottom wall of the rectangular waveguide. Some place is set to be transparent for convenient viewing. The parameters are the same with that in Fig. 2.

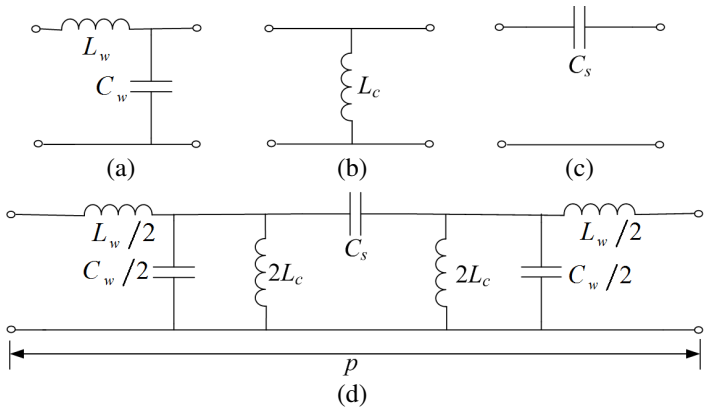

Figure 4. Equivalent circuit model of the unit cell and its component parts. (a) Equivalent circuit of rectangular waveguide. (b) Equivalent circuit of corrugations. (c) Equivalent circuit of short-ended stub. (d) Equivalent circuit model of unit cell.

at TE mode [19], which is exhibited in Fig. 4(a). When the rectangular waveguide operates at TE_{10} mode, the corrugations on both sidewalls of rectangular waveguide will introduce a per-unit-length shunt inductance L_c [20], as shown in Fig. 4(b).

Since there has been a shunt inductance L_c, only a considerable series capacitance is required to support left-handed (LH) propagating waves. According to the transmission line theory [21], a per-unit-length series capacitance C_s can be obtained by introducing a short-ended stub with its length slightly greater than a quarter of its guide wavelength when operating above cutoff. The short-ended stub is attached on the bottom wall of rectangular waveguide, and its equivalent circuit model is depicted in Fig. 4(c).

Hence series inductance L_w, shunt capacitance C_w, shunt inductance L_c and series capacitance C_s, which a general model of CRLH TL consists of [1, 2], have been all obtained. The propagation constant of proposed CRLH waveguide can be gotten using the Bolch-Floquet theorem. Certain frequency ranges of LH and right-handed (RH) passband will appear with properly choosing parameters.

2.3. Dispersion Characteristic

In order to get an accurate dispersion diagram of the improved CRLH waveguide unit cell, the 3-D finite element method (FEM) software HFSS has been chosen to simulate the structure. By using HFSS

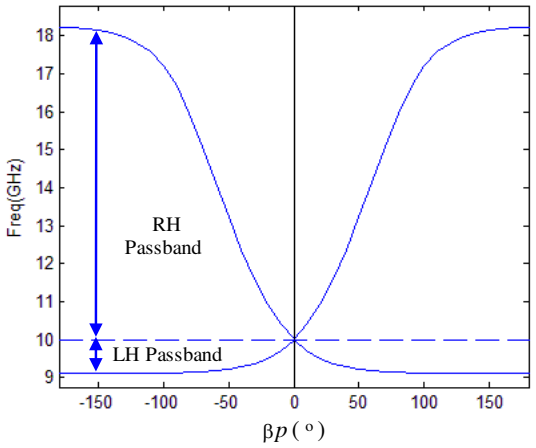

Figure 5. Dispersion diagram of the improved CRLH waveguide unit cell from HFSS simulations. 10 GHz is the infinite wavelength frequency.

eigenmode, we can simulate one-unit cell (unit cell A or unit cell B) with master and slave boundaries which enable you to model planes of periodicity where the E-field on one surface matches the E-field on another to within a phase difference. The master and slave boundaries force the E-field at each point on the slave boundary match the E-field to within a phase difference at each corresponding point on the master boundary [22]. The dispersion diagram is depicted in Fig. 5, employing the parameters given in Fig. 2. It can be seen from the dispersion diagram that, the LH passband is between 9.1 and 10 GHz, while the RH passband is between 10 and 18.2 GHz. There is no bandgap between the LH and RH passband, and 10 GHz is *the infinite wavelength frequency*. When the CRLH waveguide operates at the infinite wavelength frequency, all the slot elements cut along the waveguide wall are excited in-phase. This feature makes it feasible to introduce space variation into the design of resonant slotted-waveguide antenna array.

2.4. Transmission Characteristic

HFSS driven modal simulation of twenty-unit structure is carried out, including two sections of R100 waveguide connected at both ends, as shown in Fig. 6 (inset). The unit cell used here is also with the parameters given in Fig. 2. The scattering parameters magnitude (S_{11} and S_{21}) are plotted in Fig. 6. From the figure, we can see that the forbidden band between the LH and RH passband disappears. It can

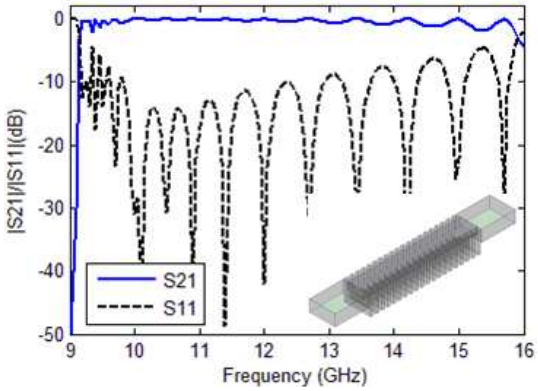

Figure 6. Scattering parameters of the twenty-unit structure with two R100 waveguides connected at both ends.

be also found that the R100 waveguide matches the proposed CRLH waveguide quite well within a large bandwidth, including the infinite wavelength frequency ($S_{11} = -31\,\text{dB}$ @ $10\,\text{GHz}$).

3. UNEQUALLY SPACED AND EXCITED RESONANT SLOTTED-WAVEGUIDE ANTENNA ARRAY

As for the conventional resonant slotted-waveguide antenna array, there is a constraint upon the adjacent element spacing requiring that they be equal to $\lambda_g/2$, so the radiation pattern can only be tailored by the excitations of slot elements. However, by employing the infinite wavelength propagation property of the proposed CRLH waveguide, both the spacings and excitations can be introduced into the antenna design. In this section, the proposed CRLH waveguide is applied to realize unequally spaced and excited resonant slotted-waveguide antenna arrays.

3.1. Slot and Its Radiation Mechanism

To determine which kind of slot to used, the surface current distribution of the CRLH waveguide wall should be known. For a resonant slotted-waveguide array, one end of CRLH waveguide should be shorted by a metal wall to create a standing wave inside. An illustration of the surface current on CRLH waveguide wall is shown in Fig. 7. The boundary condition introduced by the metal wall forces the surface current to be always uniformly towards the longitudinal

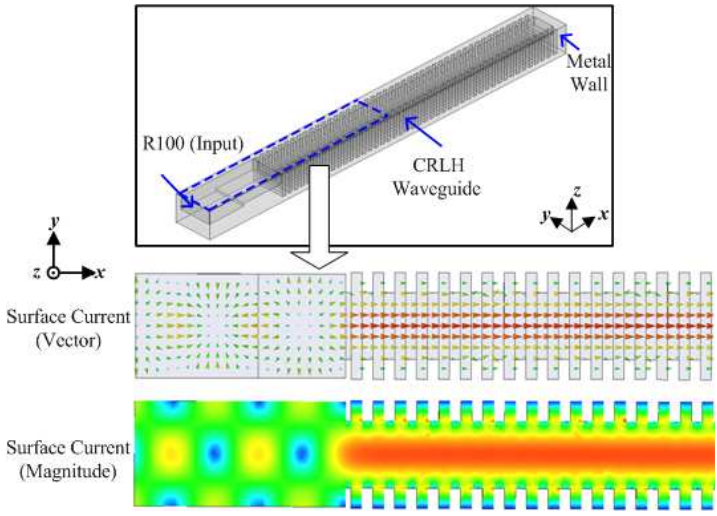

Figure 7. Illustration of a standing wave in the shorted CRLH waveguides with the mapping of the surface current. The CRLH waveguides are excited by an end-fed structure with R100 waveguide as an input port.

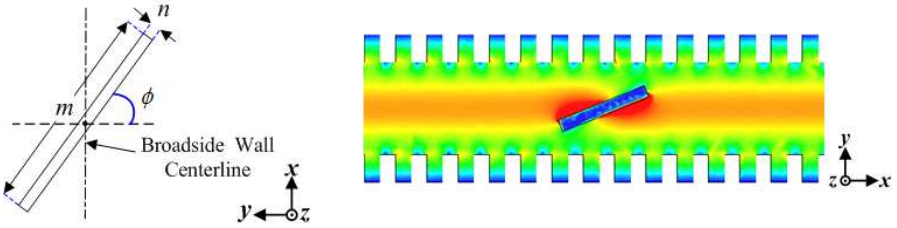

Figure 8. Slot used in this paper and its radiation mechanism. (a) Geometry and parameters of the slot (m = 14.8 mm and n = 2 mm). (b) Surface current interruption by the slot.

direction, as shown in Fig. 7. It can be seen that the wavelength is infinite long now in the CRLH waveguide.

Considering the surface current on the shorted CRLH waveguide wall, centered rotated slot with rectangular shape on the broadside wall is used in this paper, as shown in Fig. 8(a). The excitation of slot is controllable primarily by adjusting the rotation angle ϕ, and approximately proportional to $\cos\phi$. For the slot is resonant, its total length m is close to $\lambda_0/2$ (30 mm). Fig. 8(b) shows the slot interrupts

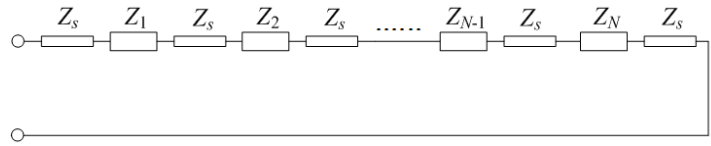

Figure 9. Transmission line circuit model of the proposed antenna array. Z_i ($i = 1, 2, \ldots, N$) and Z_s represent the ith series impedances of the slot and the characteristic impedance of CRLH waveguide, respectively.

surface current on the CRLH waveguide wall. It can be found from the figure that the wavelength is still infinitely long. Thus the effect on the propagation when cutting resonant slots on the CRLH waveguide can be neglected, and anywhere the slots cut along the CRLH waveguide wall are excited in the same phase.

As for the impedance characteristic of the slot, the forward scattering from the slot is opposite in phase to that of the backscattered field, and hence it is modeled as a series lumped element [23]. The transmission line circuit model of the antenna array is shown in Fig. 9. To achieve an input match for an end-fed standing-wave array, the total series impedances $\sum_{i=1}^{N} Z_i$ should sum to the characteristic impedance of CRLH waveguide Z_s. However, unlike the conventional rectangular waveguide, accurately calculating the impedance of slot with respect to the rotation angle is not easy, as there are many modes within the CRLH waveguide. In this paper, if it is a small array, manually setting the rotation angles is an effective way to get a low VSWR. Some mismatch caused can be improved by tuning the dimensions of a matching waveguide between the input and the CRLH waveguide (see Fig. 1).

3.2. Synthesis of Spacing and Excitation Amplitude

For the pattern synthesis, sidelobe reduction is typically obtained by tapering the amplitude distribution. However amplitude tapering has some severe penalties, such as reduced aperture efficiency [24]. Generally speaking, the more the amplitude tapers, the smaller the aperture efficiency is. For a uniform taper, it has the best aperture efficiency, however relatively high sidelobes. Consequently, a constraint on excitation amplitudes (i.e., dynamic range ratio (DRR)), is taken into account in this paper. It is predefined to a small value during synthesis, as a small DRR is desirable to allow a better control of the amplitude tapering and to achieve a relatively high aperture efficiency.

For the unequally spaced and excited array, it has more degrees of freedom than a similar array with equally spaced elements. Therefore the unequally spaced array produces better performances than an equally spaced array with the same element number [15]. Hence forth, the synthesis objective of this paper is to synthesize an unequally spaced array which produces a better pattern performance (lower PSLL) with the same number of elements. The pattern shape applied in this paper is chosen as the pencil beam, because it is the most common pattern. However, the other pattern shapes, such as the flat top pattern, are also capable of verifying this advantage.

A synthesis code based on exhaustive search is implemented to yield appropriate element spacing and excitations. Because it is accurate but slow, exhaustive search is suitable for a small array to verify the advantages of unequally spaced and excited array. During the synthesis, the element factor is considered since it is crucial to a small array. The element factor is obtained from an antenna with single element cut on the CRLH waveguide by HFSS simulation. For simplicity, the mutual coupling among the slot element is neglected. A seven-element symmetrically situated and excited array, which is equally spaced and working at 10 GHz, is synthesized for comparison at first. Unlike our previous paper [13], the adjacent element spacings of this equally spaced array can be optimized. There are five variables for this array, which can be expressed as $\mathbf{a} = [a_1,\ a_2,\ a_3,\ a_4]$ and d, respectively. Then another seven-element unequally spaced and excited array is synthesized, in order to get a lower PSLL. There are seven variables for this unequally spaced array, which can be expressed as $\mathbf{a} = [a_1,\ a_2,\ a_3,\ a_4]$ and $\mathbf{d} = [d_1,\ d_2,\ d_3]$, respectively. The DRRs of two antenna arrays above are both set to be 2.

3.3. Realization of Unequally Spaced and Excited Antenna Array

Using the data obtained from synthesis, these two different resonant slotted-waveguide antenna arrays are simulated by HFSS. To verify the advantages of the unequally spaced array, a prototype of the proposed antenna arrays is realized as shown in Fig. 10. The material of CRLH waveguide used is brass. The input waveguide R100 is connected with a standard coaxial-waveguide transformer.

Far-field radiation pattern of the fabricated antenna array is measured, and compared with the FEM simulated results, as shown in Fig. 11. Some data of two different resonant slotted-waveguide antenna arrays are summarized in Table 1. In the H-plane, as given in Fig. 11(a), it is observed that radiation patterns of equally spaced array and unequally spaced array are almost the same. The measured

Figure 10. Prototype of a seven-element unequally spaced and excited resonant slotted-waveguide antenna array.

Table 1. Comparison of equally spaced and unequally spaced arrays.

Array Type	Element Spacing	Amplitude/ Rotation Angle	$BW_{3\,\mathrm{dB}}$	PSLL
Equally Spaced Array (Synthesis)	All element spacings d_i are equal to $0.71\lambda_0$	$\mathbf{a} = [1, 0.930, 0.670, 0.500]$	6.0°	$-21.8\,\mathrm{dB}$
Unequally Spaced Array (Synthesis)	$\mathbf{d} = [0.655, 0.735, 0.820]\lambda_0$	$\mathbf{a} = [1, 1.000, 0.820, 0.500]$	6.0°	$-25.2\,\mathrm{dB}$
Unequally Spaced Array (Simulation)	$\mathbf{d} = [0.655, 0.735, 0.820]\lambda_0$	$\boldsymbol{\phi} = [75, 76, 79, 84]^\circ$	6.0°	$-24.1\,\mathrm{dB}$
Unequally Spaced Array (Experiment)	$\mathbf{d} = [0.655, 0.735, 0.820]\lambda_0$	$\boldsymbol{\phi} = [75, 76, 79, 84]^\circ$	6.6°	$-16.5\,\mathrm{dB}$

radiation pattern of unequally spaced array on H-plane matches the simulated result well.

E-plane far-field radiation patterns are shown in Fig. 11(b). From the synthesis results, it can be found that the proposed antenna array produces a 3.4 dB lower PSLL than the equally spaced antenna array does. This result indicates that the unequally spaced and excited array has advantages over the equally spaced but unequally excited array. The simulated PSLL is a little lower (1.1 dB) than the synthesized PSLL for the unequally spaced array, and it may be because of the effect of mutual coupling among the slots. For the measured results, the fabricated antenna array produces a broadside beam ($\theta = 0^\circ$), which

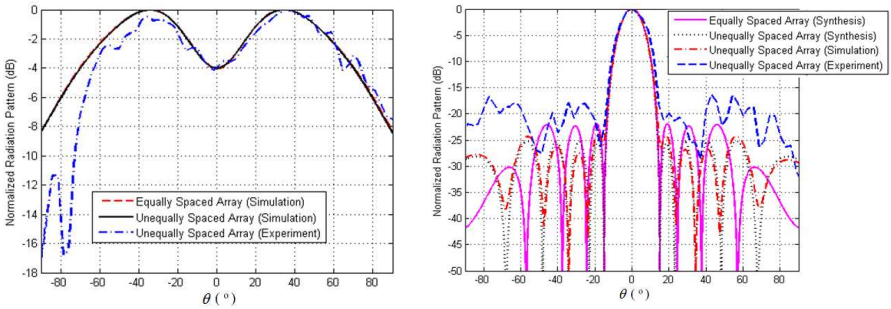

(a) (b)

Figure 11. Comparison of far-field radiation patterns between the equally spaced and unequally spaced arrays. (Freq = 10 GHz). (a) H-plane (y-z plane, $\phi = 90°$) (b) E-plane (x-z plane, $\phi = 0°$).

confirms that the slots cut along CRLH waveguide wall are excited in the same phase. However, the experimental results (especially for the value of PSLL) are some different from the simulated results. This may be due to the fact that the element factors in the simulated environment and the testing environment are not exactly the same. According to the principle of pattern multiplication, little deviation of element factor will cause differences in the radiation patterns, especially for small arrays. If it is a large array which is not susceptible to the element factor, a good agreement between the simulated and measured results may be achieved.

4. CONCLUSION

In this paper, a new concept of unequally spaced and excited resonant slotted-waveguide antenna array has been proposed. It was realized by employing an improved resonant-slot coupled cavity chain CRLH waveguide. By utilizing the infinite wavelength propagation property of the proposed CRLH waveguide, the spacings, as well as the excitation amplitudes have been introduced into the array synthesis. To conclude, the results show that when compared with the equally spaced array, the proposed antenna array produces a lower PSLL for same number of elements.

It is worth noticing that, the advantage demonstrated by small arrays, is much more significant for large arrays. Also, the advantage is attractive when the new type of array is applied to the other pattern shapes, such as the flat top pattern.

ACKNOWLEDGMENT

This work was supported by the Chinese Natural Science Foundation under Contract 60871057.

REFERENCES

1. Caloz, C. and T. Itoh, *Electromagnetic Metamaterials: Transmission Line Theory and Microwave Applications*, Wiley-IEEE Press, 2005.
2. Eleftheriades, G. V. and K. G. Balmain, *Negative-Refraction Metamaterials: Fundamental Principles and Applications*, Wiley-IEEE Press, 2005.
3. Eshrah, I. A., et al., "Rectangular waveguide with dielectric-filled corrugations supporting backward waves," *IEEE Trans. Antennas Propag.*, Vol. 53, No. 11, 3298–3304, Nov. 2005.
4. Liao, S., P. Yan, J. Xu, et al., "Left-handed transmission line based on resonant slot coupled cavity chain," *IEEE Microw. Wireless Compon. Lett.*, Vol. 17, No. 4, 292–294, Apr. 2007.
5. Ueda, T., et al., "Dielectric-resonator-based composite right/left-handed transmission lines and their application to leaky wave antenna," *IEEE Trans. Microw. Theory Tech.*, Vol. 56, No. 10, 2259–2269, Oct. 2008.
6. Ikeda, T., et al., "Beam-scanning performance of leaky-wave slot-antenna array on variable stub-loaded left-handed waveguide," *IEEE Trans. Antennas Propag.*, Vol. 56, No. 12, 3611–3618, Dec. 2008.
7. Abdelaziz, A. F., et al., "Realization of composite right/left-handed transmission line using coupled lines," *Progress In Electromagnetics Research*, Vol. 92, 299–315, 2009.
8. Monti, G., R. De Paolis, and L. Tarricone, "Design of a 3-state reconfigurable CRLH transmission line based on MEMS switches," *Progress In Electromagnetics Research*, Vol. 95, 283–297, 2009.
9. Jimenez-Martin, J. L., et al., "Dual band high efficiency class CE power amplifier based on CRLH diplexer," *Progress In Electromagnetics Research*, Vol. 97, 217–240, 2009.
10. De Castro-Galan, D., L. E. Garcia Munoz, D. Segovia-Vargas, and V. Gonzalez-Posadas, "Diversity monopulse antenna based on a dual-frequency and dual mode CRLH ratrace coupler," *Progress In Electromagnetics Research B*, Vol. 14, 87–106, 2009.
11. Si, L.-M. and X. Lv, "CPW-fed multi-band omni-directional planar microstrip antenna using composite metamaterial resonators

for wireless communications," *Progress In Electromagnetics Research*, Vol. 83, 133–146, 2008.

12. Yu, A., F. Yang, and A. Elsherbeni, "A dual band circularly polarized ring antenna based on composite right and left handed metamaterials," *Progress In Electromagnetics Research*, Vol. 78, 73–81, 2008.
13. Liao, S., Y. Chen, J. Wei, and J. Xu, "Unequally spaced resonant slotted-waveguide antenna array based on the infinite wavelength propagation property of composite right/left-handed waveguide," *IEEE Antennas and Wireless Propag. Lett.*, Vol. 9, 451–454, 2010.
14. Hrabar, S., H. Kumric, and D. Zaluski, "Investigation of guiding and radiating properties of resonant-slot coupled cavity chain," *3rd European Conference on Antennas and Propagation*, 3147–3150, 2009.
15. Unz, H., "Linear arrays with arbitrarily distributed elements," *IEEE Trans. Antennas Propaga.*, Vol. 8, 222–223, Mar. 1960.
16. Kumar, B. P. and G. R. Branner, "Design of unequally spaced arrays for performance improvement," *IEEE Trans. Antennas Propag.*, Vol. 47, No. 3, 511–523, Mar. 1999.
17. Allen, M. A. and G. S. Kino, "On the theory of strongly coupled cavity chains," *IEEE Trans. Microw. Theory Tech.*, Vol. 8, No. 3, 362–372, May 1960.
18. Bevensee, R. M., "Propagation in the helical and narrow-band slow wave structures," *IRE Trans. on Electron Devices*, Vol. 8, No. 6, 549–558, 1961.
19. Ramo, S., J. R. Whinnery, and T. V. Duzer, *Fields and Waves in Communication Electronics*, John Wiley & Sons, Inc., 1994.
20. Marcuvitz, N., *Waveguide Handbook: Four-terminal Structures*, Peter Peregrinus, 1986.
21. Pozar, D. M., *Microwave Engineering*, 3rd edition, John Wiley & Sons, Inc., 2005.
22. HFSS, Version 12.0.0, Ansoft Corporation, Pittsburgh, USA, 2009.
23. Milligan, T. A., *Modern Antenna Design*, 2nd edition, John Wiley & Sons, Inc., 2005.
24. Bhattacharyya, A. K., *Phased Array Antennas*, John Wiley & Sons, Inc., 2006.